THERMO-VISCOELASTIC MODEL FOR THE CONTRACTION DURING THE POLYMERIZATION OF BULK FILL RESINS

Claudio Antunes Junior, Universidade Federal do Paraná, cantunes.j@gmail.com
Emílio Graciliano Ferreira Mercuri, Universidade Federal do Paraná, emilio@ufpr.br
Ana Paula Gebert Oliveira Franco, Universidade Tecnológica Federal do Paraná, anapaula.gebert@gmail.com
Leandro Zen Karam, Pontifícia Universidade Católica do Paraná, leandro.karam@pucpr.br
Manoella Costa, Universidade Estadual de Ponta Grossa, costa.manoella@hotmail.com

Resumo. *The objective of this work is to do a comparison between the thermo-viscoelastic model that uses Prony series with the laboratory experiment that is about the contraction of bulk fill resins during its polymerization, in order to avoid failure in the interface between the resin and dentin, such as micro-infiltrations that can lead to other problems. The laboratory experiment was done in third human molars, in which were installed an optical fiber with two FBG sensors that measure strain and temperature. For the computational model, a first human molar model was used, the simulation was performed in Ansys software and the input data was the temperature measured by one of the sensors during the polymerization process. The results obtained are promising, however, it is still necessary to do a better treatment in the pairs values of the Prony series to represent in fact the slow deformation suffered by the resin.*

Palavras chave*: Bulk-fill Resin. FEM. Prony Series. Contraction. Thermo-viscoelastic.*

1. INTRODUCTION

Composite resins of the bulk fill type were developed in order to facilitate the restoration process, since its recommended increment is usually 4 mm of depth, twice as much as the depth of the increment that is traditionally used with conventional resins (Benetti et al., 2015; Zorzin et al., 2015). It should also be considered that recently developed bulk-fill resins have lower volumetric contraction and consequently lower residual stress from the contraction process caused by the polymerization (Ilie and Hickel, 2011). However, the availability of the properties of these resins is limited (Walter, 2013).

The high contraction of the composite dental resins caused by the process of polymerization during the restoration may cause defects in the interface between the resin and dentin. This failure can entail a micro-infiltration problem, which can lead to the development of postoperative sensitivity, pulp damage and the return of caries. With the high contraction, even the loss of the restoration can occur (Benetti et al., 2015; Lutz et al., 1991; Zorzin et al., 2015).

The objective of this work is to do a comparison between the thermo-viscoelastic constitutive model, that uses Prony series with the laboratory experiment. It is necessary to point out that the model is in its initial calibration process of the Prony constants. The model that was used represents the polymerization strain in bulk-fill composite resins, to avoid the problems that the high contraction can cause and the economic impact due to the necessity of investments to restore the damage tooth, due to the repetition. To accomplish this the authors developed a computational experiment to compare the results with a laboratorial experiment.

With the numerical model validation, it will be used to study different light exposition patterns and the depth of the resin apposition, procedures that are critical during the restoration process.

2. LINEAR VISCOELASTIC MODEL

The linear viscoelastic constitutive models are commonly represented by simple physical models which are composed of springs and dashpots. The spring is the linear-elastic component and the dashpot is the viscous components, the constitutive equations are Eq. (1) and Eq. (2), respectively (Findley et al., 1989).

$$\sigma = E \cdot \varepsilon \tag{1}$$

$$\sigma = \eta \cdot \frac{\partial \varepsilon}{\partial t} \tag{2}$$

Being σ the stress, E the Young's modulus, ε the strain and η the viscosity constant. The constitutive models like Maxwell, Kelvin and Burgers are constructed by the parallel and/or series of combinations of springs and dashpots (Findley et al., 1989).

3. VISCOELASTIC MODEL WITH PRONY SERIES

The viscoelastic constitutive model is based on the generalized Maxwell model for three dimensions, which is constituted by a spring element in parallel with n spring and dashpot Maxwell elements, is given by Eq. (3) (SAS IP, Inc).

$$\sigma = \int_0^t 2G(t-\tau)\frac{d\varepsilon}{d\tau}d\tau + I\int_0^t K(t-\tau)\frac{d\Delta}{d\tau}d\tau \tag{3}$$

Being σ the stress tensor, ε the strain tensor, Δ the volumetric strain, I the identity tensor and τ the past time. Where G(t) and K(t) are the Prony series shear and bulk modulus, respectively. Those are represented by the Eq. (4) and (5) (SAS IP, Inc).

$$G(t) = G_0\left[\alpha_\infty^G + \sum_{i=1}^{n_G}\alpha_\infty^G e^{\left(-\frac{t}{\tau_i^G}\right)}\right] \tag{4}$$

$$K(t) = K_0\left[\alpha_\infty^K + \sum_{i=1}^{n_K}\alpha_\infty^K e^{\left(-\frac{t}{\tau_i^K}\right)}\right] \tag{5}$$

Where G_0 and K_0 are the relaxation modules at t = 0, n_G and n_K are the number of Prony pairs, α_i^G and α_i^K are the relative modulus and τ_i^G and α_i^K are the relaxation times (SAS IP, Inc).

4. THERMOELASTIC MODEL

Based on the Hooke's 3D law and the isotropic thermoelastic effects. The change in the temperature ΔT has a volumetric influence in the stress level. The relation between strain and stress is shown in Eq. (6).

$$\sigma_{ij} = C_{ijkl}\cdot\left(\varepsilon_{kl}^e - \varepsilon_{kl}^T\right) = C_{ijkl}\cdot\left(\varepsilon_{kl}^e - \alpha\Delta T\delta_{kl}\right) \tag{6}$$

Where C_{ijkl} is the fourth-order stiffness tensor and α is the isotropic coefficient of thermal expansion. The ε_{kl}^e and ε_{kl}^T are the second-order elastic strain and thermal strain tensors, σ_{ij} is the second-order stress tensor and δ_{kl} is the Kronecker delta tensor (Radovitzky et al., 2013).

5. THERMO-VISCOELASTIC MODEL

The thermo-viscoelastic model used in the simulation is a combination of Equations (3) and (6) and is represented by the Eq. (7) (Christensen, 2012).

$$\sigma_{ij} = \int_0^t 2G_{ijkl}(t-\tau)\frac{d\varepsilon_{kl}}{d\tau}d\tau + I_{ijkl}\int_0^t K(t-\tau)\frac{d\Delta_{kl}}{d\tau}d\tau - C_{ijkl}\alpha\,\Delta T\,\delta_{kl} \tag{7}$$

6. MATERIALS AND METHODS

The experiment was done at the thermography laboratory of the Federal Technological University of Paraná, which had a controlled temperature of 21ºC when the experiment was performed. Were used 15 samples of third human molars free of dental cavities in the experiment that were fixated in resin, in each one a cavity of 4x4x4 mm and two through holes that are perpendicular to each other at 2 and 3 mm of the bottom of the cavity were created. In these holes an optical fiber recorded with two fiber Bragg grating (FBG) sensors was inserted, one of them was inside a hypodermic needle. After the positioning of the sensors the cavity was filled with the Filtek Bulk Fill Flow resin (3M/ESPE) and then photoactivated for 10 seconds with the LED device (Vallo Cordless/Ultradent). A representation of the laboratory experiment can be seen in the photography illustrated by Fig. (1).

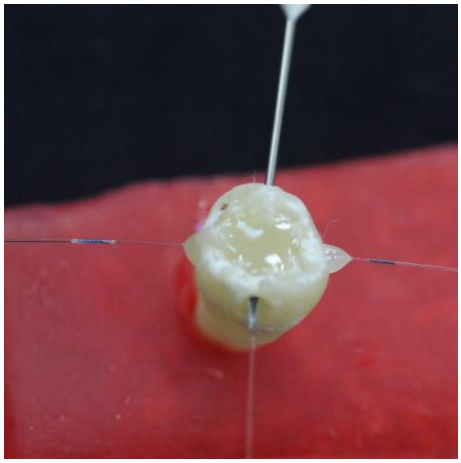

Figure 1. Photography of the laboratory experiment

The two FBG sensors were used to measure the strain and temperature during the polymerization of the resin. The sensors at 2 and 3 mm of the bottom of the cavity, measured, strain and temperature, and only temperature due to the use of the hypodermic needle, respectively. The measurements were recorded every half second for one hour and analyzed statistically and converted to temperature and strain, this conversion was necessary because the recorded data is in wavelength. The authors choose one sample of the 15 samples of third human molars, that has the smoothest curves with the median values compared to the others tests, so it can be used in the computational model. This choice is shown in Fig. (2).

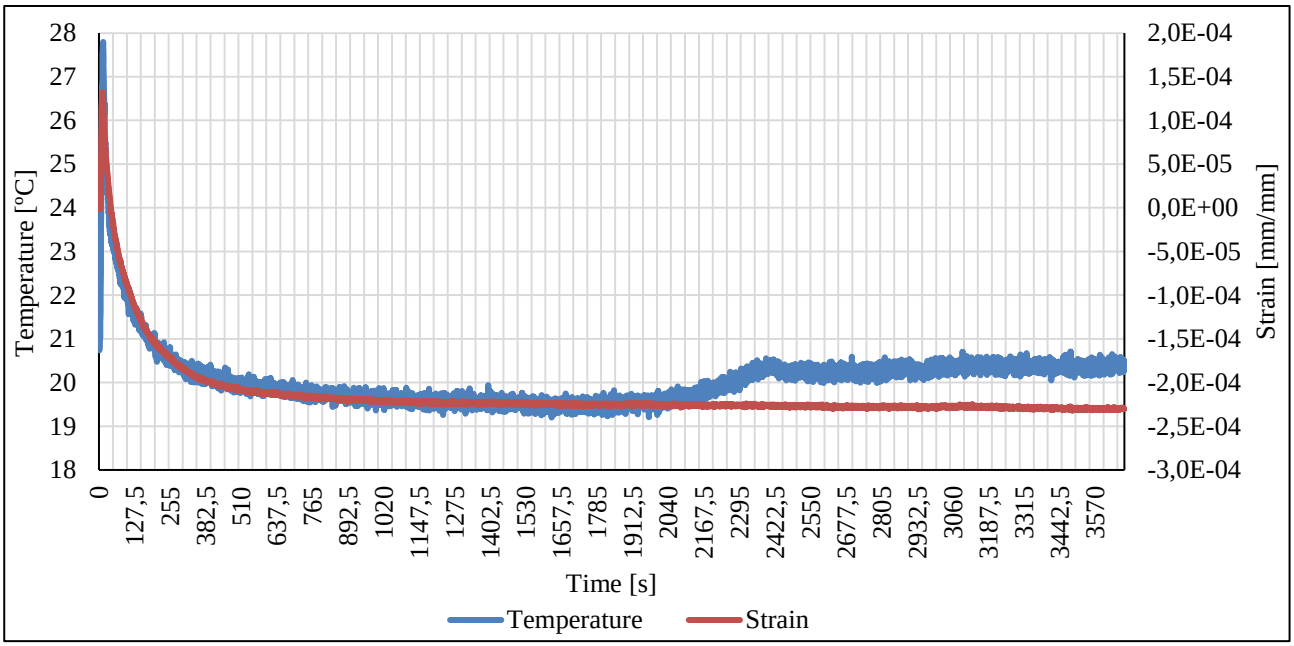

Figure 2. Temperature and strain evolution during polymerization

For the computational model a three-dimensional model of a first human molar obtained by a CT scan was used. With the FreeCad software, a cavity with 4x4x4 mm dimensions was created. The cavity was filled with dental resin model, which has the upper surface equal as the one on the first molar complete model. In order to apply the boundary conditions in the model, it was necessary to create a model that simulate the bulk cortical bone. It is important to emphasize that the geometry of the model is in the initial state and is simplified, it will be improved by replacing the first molar with a third human molar that was used in the laboratory experiment by a CT scan.

Afterwards a static structure analysis using the finite element method was performed with the software Ansys. To start the analysis was necessary to define the properties of the components of the model as shown in Tab. (1). The dentin and cortical bone were considered as linear elastic and isotropic materials. For the resin it was considered as a viscoelastic material represented by the Prony series bulk constants, the relaxation time was 1, 10 and 10^5 and the relative modulus was 0.01, 0.1 and 0.8, those values were chosen arbitrarily.

Table 1. Properties of the components

Material	Young Modulus E [MPa]	Poisson Coefficient ν	Coefficient of Thermal Expansion [°C^{-1}]
Dentin	18600 [a]	0,31 [a]	20E-5 [c]
Cortical Bone	13700 [a]	0,30 [a]	10E-5 [d]
Dental Resin	3700 [e]	0,25 [b]	5E-5 [c]

[a] Boccacio et al., 2006. [b] Xu et al., 1999. [c] Alnazzawi et al., 2012. [d] Ranu, 1987. [e] Leprince et al., 2014.

After this the contact regions of the components that are bonded were defined, which are between the tooth roots and the cortical bone and between the tooth cavity and the dental resin. The boundary condition that was used is the no displacement for the inferior face of the cortical bone model. Figure (3) shows the contact regions and the boundary condition.

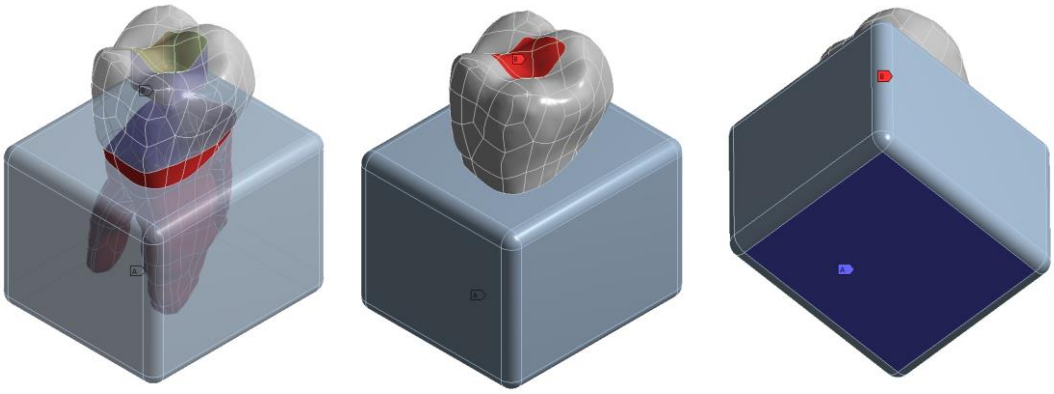

Figure 3. Representation of the contact regions, thermal load and boundary condition

The thermal load that was used is based on the temperature that was measured during the laboratory experiment that was shown in Fig. (2) and it was only applied to the resin model is represented by Fig. (3). However, in the experiment more than 7000 measurements were made, due to this it was decided to use the temperature data every two seconds for the first 200 seconds.

For the mesh, it was used the Tetrahedrons geometry with the element size of 1 mm and the element order as quadratic (Antunes Junior, 2017). The element size is not smaller at the resin model, because of the computational time that is already required to do the analysis is high, and the computer that was used can't handle more refined meshes.

To compare the laboratory experiment and the computational model results, a probe was created at 2 mm from the bottom of the resin model, so it could simulate the FBG sensor. Figure (4) shows the position of the probe by the axes.

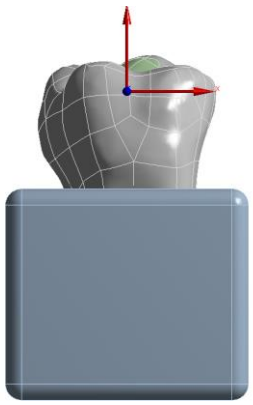

Figure 4. The blue dot represents the probe that is located in the same region of the FBG sensor

After all these steps, the system is solved one time using the thermoelastic model and multiple times with the thermo-viscoelastic model with Prony series constants that were arbitrary, obtaining the deformation of the point during the polymerization process.

7. RESULTS

Before determining the elastic modulus that would be used as a property of the bulk fill resin, two tests were performed using 3GPa (Xu et al., 1999) and 3,7GPa (Leprince et al., 2014) for the elastic modulus with the thermoelastic model, the results can be seen in Fig. (5).

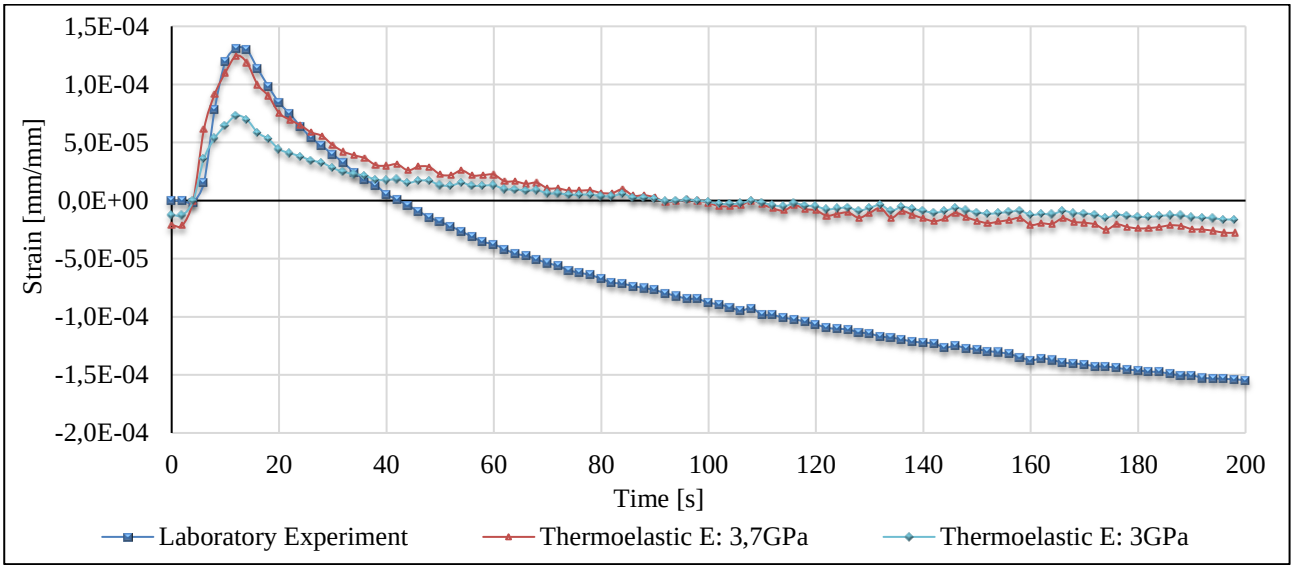

Figure 5. Influence of the elastic modulus in the strain evolution

As can be seen the modulus of elasticity has a major impact in the first 20 seconds of the deformation, where the elastic deformation occurs. Note that when using the 3.7GPa modulus we almost get the same peak obtained in the laboratory experiment, but still more adjustments are needed, since the initial 5 seconds in the computational model already exists deformation differently from the laboratory experiment, where there is none.

The results that were found for the strain on the probe using the thermoelastic and the Prony series models with the strain data from the laboratory experiment were set out in Fig. (6).

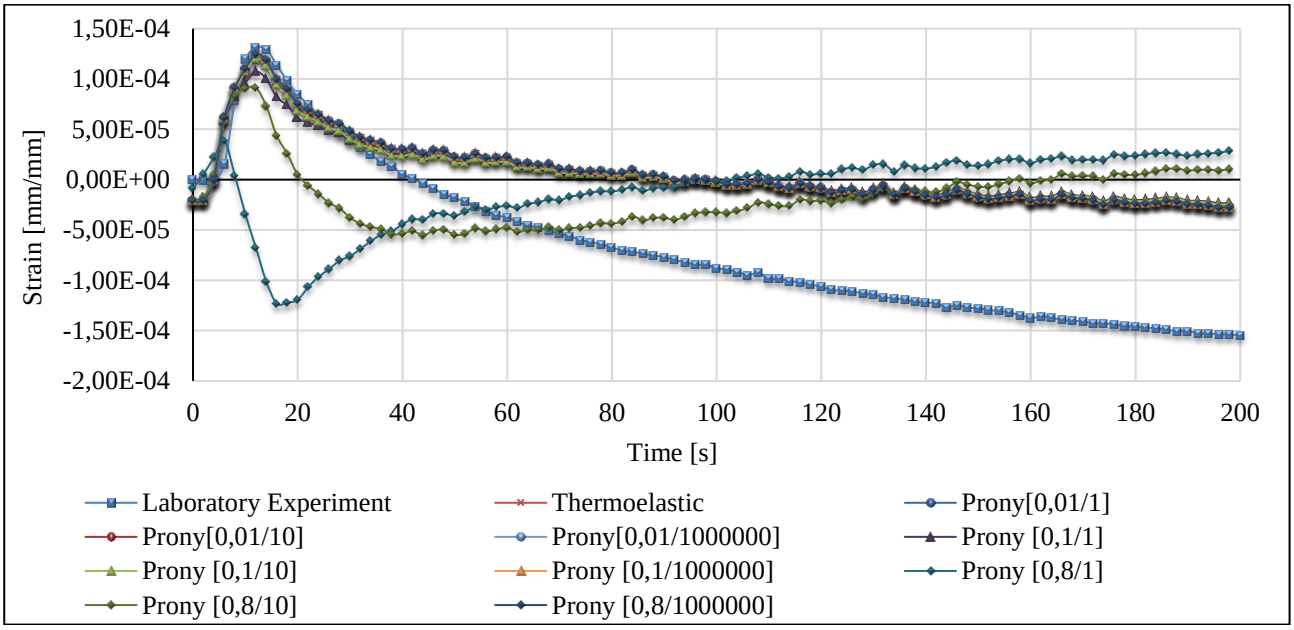

Figure 6. Comparison between models of the strain evolution

According to the Fig. (6) both of the thermoelastic and viscoelastic models that were used were not able to reproduce the result obtained in the laboratory experiment. It is seen that the great part of the pairs of Prony series that were used

presented results close to the thermoelastic model. However, the pairs 0.8 / 1 and 0.8 / 10^5 had unusual results, did not even represented the elastic deformation properly. Among the other results only the 0.01 / 1 pair had its peak slightly below the others in the elastic deformation. All the pairs used were not able to represent the slow deformation suffered by the resin during its polymerization.

8. CONCLUSION

Although the objective of replicating the behavior of the resin during its polymerization has not been reached through the use of the thermoelastic model or viscoelastic model with Prony series, it was at least possible to verify that the elastic modulus has a great influence to find the elastic deformation. It was also possible to verify that the values of the pairs for the Prony series that were used are not sufficient to find the slow deformation suffered by the resin. Furthermore, the authors will divide the curve of the strain obtained from the laboratory experiment to find the pairs that best describe the viscoelastic properties of the resin, by using Eq. (4) and (5). In general, the work contributes to the study of models that can be applied in order to represent the contraction of bulk fill resins in order to avoid unnecessary expenses.

9. REFERENCES

ANTUNES JUNIOR, C.; MERCURI, E.G.F. Estudo de convergência de malha para modelo representativo de molar submetido a cargas de mastigação. In: SIMPÓSIO DE MÉTODOS NUMÉRICOS EM ENGENHARIA, 2, Curitiba, 2017. **Anais do II Simpósio de Métodos Numéricos em Engenharia**, Curitiba: Setor de Tecnologia da UFPR, v. 1, p. 304-308, 2017.

BENETTI, A.R.; HAVNDRUP-PEDERSEN, C.; HONORÉ, D.; PEDERSEN, M.K.; PALLESEN, U. Bulk-fill resin composites: polymerization contraction, depth of cure, and gap formation. **Operative Dentistry**, v. 40, p. 190-200, 2015.

BOCCACIO, A.; LAMBERTI, L.; PAPPALETTERE, C.; CARANO, A.; COZZANI, M. Mechanical behavior of an osteotomized mandible with distraction orthodontic devices. **Journal of Biomechanics**, v. 15, p. 2907-2918, 2006.

CHRISTENSEN, R. Theory of viscoelasticity: an introduction. **Elsevier**, 2012.

FINDLEY, W.N.; LAI, J.S.; ONARAN, K. Creep and relaxation of nonlinear viscoelastic materials: with and introduction to linear viscoelasticity. New York: **Dover Publications**, 1989.

ILIE, N.; HICKEL, R. Investigations on a methacrylate-based flowable composite based on the SDR technology. **Dental Materials**, v. 27, p. 348-355, 2011.

LEPRINCE, J.G.; PALIN, W.M.; VANACKER, J. et al. Physico-mechanical characteristics of commercially available bulk-fill composites. **Journal of Dentistry**, v. 42, p. 993-1000, 2014.

LUTZ, F.; KREJCI, I.; BARBAKOW, F. Quality and durability of marginal adaptation in bonded composite restorations. **Dental Materials**, v. 7, p. 107-113, 1991.

RADOVITZKY, R.; HAUTEFEUILLE, M.; JEAN, A.; ROSOLÉM, A.; BECKER, G. Structural mechanics: module 3. Available at: <http://web.mit.edu/16.20/homepage/3_Constitutive/Constitutive_files/module_3_no_solutions.pdf>. Accessed in: 27 aug. 2017.

RANU, H.S. The thermal properties of human cortical bone: an in vitro study. **Journal of Engineering in Medicine**, v. 16, p. 175-176, 1987.

SAS IP, Inc. 3.7. Viscoelasticity. Available at: <https://www.sharcnet.ca/Software/Ansys/16.2.3/en-us/help/ans_mat/evis.html#mat_viscosmalldef>. Accessed in: 11 nov. 2017.

WALTER, R. Critical appraisal: bulk-fill flowable composite resins. **Journal of Esthetic and Restorative Dentistry**, v. 25, p. 72-76, 2013.

XU, H.H.K.; MARTIN, T.A.; ANTONUCCI, J.M.; EICHMILLER, F.C. Ceramic whisker reinforcement of dental resin composites. **Journal of Dental Research**, v. 78, p. 706-712, 1999.

ZORZIN, J.; MAIER, E.; HARRE, S.; FEY, T. et al. Bulk-fill resin composites: polymerization properties and extended light curing. **Dental Materials**, v. 31, p. 293-301, 2015.

10. ACKNOWLEDGEMENTS

The authors would like to acknowledge the financial support from the Coordination for the Improvement of Higher Education Personnel (CAPES), the Post-Graduate Program in Numerical Methods in Engineering (PPGMNE/UFPR) and the Laboratory of Thermography of UTFPR.

11. INFORMATION RESPONSABILITIES

The authors are solely responsible for the information included in this work.